

# Distilled Prompt Learning for Incomplete Multimodal Survival Prediction

Yingxue Xu<sup>1</sup> Fengtao Zhou<sup>1</sup> Chenyu Zhao<sup>1</sup> Yihui Wang<sup>1</sup> Can Yang<sup>2</sup> Hao Chen<sup>1</sup>✉

<sup>1</sup>Department of Computer Science and Engineering, <sup>2</sup>Department of Mathematics  
The Hong Kong University of Science and Technology

{yxueb, fzhouaf, cyzhao, ywangrm}@connect.ust.hk, {macyang, jhc}@ust.hk

## Abstract

The integration of multimodal data including pathology images and gene profiles is widely applied in precise survival prediction. Despite recent advances in multimodal survival models, collecting complete modalities for multimodal fusion still poses a significant challenge, hindering their application in clinical settings. Current approaches tackling incomplete modalities often fall short, as they typically compensate for only a limited part of the knowledge of missing modalities. To address this issue, we propose a Distilled Prompt Learning framework (*DisPro*) to utilize the strong robustness of Large Language Models (*LLMs*) to missing modalities, which employs two-stage prompting for compensation of comprehensive information for missing modalities. In the first stage, Unimodal Prompting (*UniPro*) distills the knowledge distribution of each modality, preparing for supplementing modality-specific knowledge of the missing modality in the subsequent stage. In the second stage, Multimodal Prompting (*MultiPro*) leverages available modalities as prompts for *LLMs* to infer the missing modality, which provides modality-common information. Simultaneously, the unimodal knowledge acquired in the first stage is injected into multimodal inference to compensate for the modality-specific knowledge of the missing modality. Extensive experiments covering various missing scenarios demonstrated the superiority of the proposed method. The code is available at <https://github.com/Innse/DisPro>.

## 1. Introduction

Multimodal Survival Prediction typically incorporates pathology slides and genomic data complementary to each other for precise prognosis analysis. Pathology data can provide qualitative morphological insights, while quantitative molecular information can be obtained from genomic data [5, 32, 33]. Despite progress [5, 8, 33] in multimodal survival analysis, these models typically require complete modalities data for reliable performance. However, the ex-

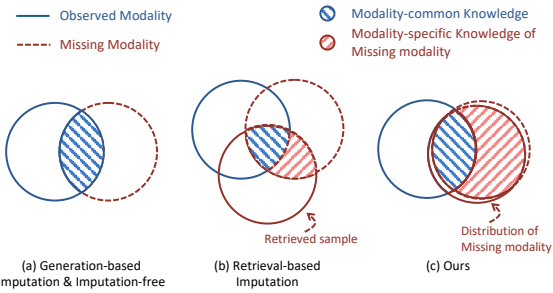


Figure 1. Insights for existing incomplete multimodal learning and comparison to the proposed method. (a) Generation-based Imputation and Imputation-free approaches, (b) Retrieved-based Imputation and (c) Ours.

pectation of having full access to complete modalities for integration is not always achievable, especially in clinical scenarios, due to various factors such as the cost of data gathering and privacy issues. For example, acquiring genomic data still comes at a high cost due to the technology and infrastructure required for gene sequencing, especially in underdeveloped areas [40]. Inevitably, it is challenging to adapt previously established multimodal survival models [27, 39] to real-world clinical settings. As a result, building a multimodal survival model that is robust to incomplete modalities data is an urgent issue for clinical practice.

Currently, mainstream approaches addressing incomplete modalities issues include imputation-based and imputation-free methods [7, 31]. The former approaches aim to impute the missing modality based on observed modalities, primarily achieved in two ways including generation [3, 20, 26] and retrieval [4, 37]. In terms of generation-based imputation, generative models are typically employed for synthesizing features or raw data of missing modalities from available modalities. As shown in Fig. 1 (a), these methods usually can only impute modality-common information, as the modality-specific information unique to the missing modality cannot be generated out of thin air. Moreover, the goal of retrieval-based imputation methods is to fill in missing modalities by seeking the most similar sample of the missing modality from the training set. This way tends

to compensate only a limited part of modality-common and modality-specific information, as shown in Fig. 1 (b). The reason is that an individual sample exhibits considerable randomness and is challenging to fully capture the unique knowledge inherent in the missing modality.

Unlike imputation-based approaches, imputation-free approaches [7, 31] primarily focus on how to minimize performance degradation resulting from missing modalities. These approaches make great efforts to learn robust multimodal representations that are less sensitive to missing modalities by capturing modality-invariant information. Recently, with the rise of Large Language Models (LLMs) [1, 17, 30], the researcher [15] attempts to leverage the strong robustness of LLMs benefit from extensive training data to alleviate performance decreases caused by incomplete modalities. They design some sophisticated prompts to inform LLMs of different distributions of inputs. However, they only capture modality-common information as well (Fig. 1a), ignoring distinct modality-specific knowledge of the missing modality. As such, existing methods still struggle to effectively incorporate the learning of both common and specific knowledge of missing modalities.

Based on these insights, to bridge the aforementioned gap, we propose a **Distilled Prompt Learning** (DisPro) framework to unlock LLMs’ robustness to incomplete modalities, which aims to simultaneously compensate for both specific and common information of missing modalities. It comprises two-stage prompt learning including Unimodal Prompting (UniPro) and Multimodal Prompting (MultiPro) for capturing modality-specific and modality-common information of missing modalities, respectively.

In the first stage, to prepare for supplementing modality-specific information of missing modalities, we first learn the knowledge distribution of the missing modality by distilling unimodal knowledge into a set of learnable unimodal prompts for each modality from all remaining samples available of this modality. Specifically, inspired by CoOp [41], a set of learnable prompts for different classes is employed to learn knowledge about how to describe different categories of an individual modality. For example, in survival prediction, learned prompts can be intuitively interpreted as how different risk groups will reflect in pathological morphology or gene expression profiles. However, due to the huge size (e.g.,  $100,000 \times 100,000$ ) of pathological WSIs, we cannot simply apply CoOp designed for small natural images to WSIs. Therefore, in UniPro, we extend CoOp into the multiple instance learning (MIL) paradigm that is commonly used for large-scale WSIs [9, 11, 34].

In the second stage, to capture modality-common information for missing modalities, we leverage available modalities as multimodal prompts of LLMs to infer representations of missing modalities using LLMs’ strong inference ability. Simultaneously, to inject the learned unimodal

knowledge in stage 1, we propose UniPro Distillation to enforce the inferred representations of missing modalities to get as close as possible to the learned unimodal prompts of the corresponding class. Additionally, to assist in learning modality-common knowledge from WSIs and genes with high information redundancy [27, 39], we propose UniPro Scoring to re-use UniPro as a grader to select discriminative and relevant tokens. As a result, both common and specific information are compensated for missing modalities under the collaboration of uni- and multimodal prompts, thus mitigating performance declines led by incomplete modalities.

It is worth noting that DisPro is proposed as a framework for addressing missing modality issues by leveraging LLMs’ power based on prompts, capable of generalizing to a wider range of domains. The contributions of this work are summarized as follows:

- We propose a Distilled Prompt Learning (DisPro) framework for incomplete multimodal survival prediction, where LLMs’ robustness to incomplete modalities is explored under two-stage prompting.
- We propose two-stage prompt learning including Unimodal Prompting and Multimodal Prompting to compensate for both modality-specific and modality-common information of missing modalities, respectively.
- Extensive experiments on five benchmark survival prediction datasets are conducted, which demonstrates significantly superior to state-of-the-art approaches.

## 2. Related Work

### 2.1. Incomplete Multimodal Learning

As stated above, incomplete multimodal learning [40] can be categorized into two types: imputation-based [4, 10, 35] and imputation-free methods [18, 22]. For example, with the success of the diffusion model [6], the research [20] attempted to apply it to MRI synthesis for missing modalities. Instead of generating raw modality data, SMIL [19] leveraged Bayesian meta-learning to impute features of missing modalities. For retrieval-based approaches, M3Care [37] filled in the missing modalities by retrieving the most similar samples from the training set. On the other hand, imputation-free approaches provided more flexible solutions, which aim to enhance the robustness of fusion and alleviate performance decrease. [7] proposed a segmentation-based regularizer to reduce the sensitivity to missing modalities. MUSE [31] utilized patients’ relationships based on graph networks to perform contrastive learning for improving the robustness to missing modalities. Recently, MAP [15] proposed missing-aware prompts to unlock the robustness of LLMs to missing modalities by indicating LLMs different missing scenarios. However, these methods typically supplemented modality-common knowledge for missing modalities.

## 2.2. Multimodal Survival Prediction

With the success of digital pathology [16, 21, 38] and sequencing techniques [23, 28], pathology and genomic data are commonly integrated to analyze survival outcomes, which have proven the superiority on precision in previous works [5, 33]. MCAT [5] proposed to leverage the interactions across modalities to guide the learning of pathology data. Based on this work, MOTCat [33] further leveraged optimal transport to capture global structure consistency across modalities. In parallel, CMTA [8] investigated the intrinsic cross-modal interactions and potential complementary information by cross-modal translation and alignment. From the perspective of information bottleneck, PIBD [39] proposed a prototypical information bottleneck for the MIL setting to select discriminative instances and disentangle multimodal knowledge for redundancy reduction. Similarly, MMP [27] utilized Gaussian Mixture Model to summarize morphological prototypes and biological pathway prototypes for these two modalities. However, all these methods assume all modalities available, inevitably leading to the difficulty of employment in clinical settings.

## 3. Method

This work aims to explore LLMs’ robustness to incomplete modalities by two-stage prompting, Unimodal Prompting (UniPro) and Multimodal Prompting (MultiPro), which capture modality-specific and modality-common information, respectively. The overview framework of the proposed method is shown in Fig. 2. First, we will introduce the problem formulation in Sec. 3.1. Then, we will detail the process of UniPro and MultiPro in Sec. 3.2 and 3.3, respectively.

### 3.1. Problem Formulation

Given a multimodal dataset consisting of  $M = 2$  modalities, we use a 2-tuple  $\mathbf{X}_n = (\mathbf{X}_n^p, \mathbf{X}_n^g)$  to represent the  $i$ -th patient data, where  $\mathbf{X}_n^p$  and  $\mathbf{X}_n^g$  are pathology and genomic data, respectively. In particular, we use the notation of tilde hat to indicate the modality is missing, e.g.,  $\widetilde{\mathbf{X}}_n^p$ .

Following the conventional setting for pathological WSIs and genomic pathways in previous works [12, 39], we formulate a WSI  $\mathbf{X}_n^p$  and a set of genomic pathways  $\mathbf{X}_n^g$  as the “bag” of instances in MIL paradigm. We denote  $\mathbf{X}_n^p = \{\mathbf{x}_{n,i}^p\}_{i=1}^{M_p}$  where each instance  $\mathbf{x}_{n,i}^p$  refers to a patch image cropped from the WSI  $\mathbf{X}_n^p$  and  $M_p$  is the patch number of this WSI. Similarly, the bag of genomic pathways can be formulated as  $\mathbf{X}_n^g = \{\mathbf{x}_{n,i}^g\}_{i=1}^{M_g}$ , in which an instance  $\mathbf{x}_{n,i}^g$  represents a pathway consisting of various gene expression values.

In survival prediction, the goal is to estimate the risk probability of an outcome event taking place before a specific time. However, this event may not always be observed, resulting in a right-censored occurrence. Therefore,

$c_n \in \{0, 1\}$  is used to denote censorship status indicating whether the outcome event is right-censored (i.e., alive) ( $c = 1$ ) or not ( $c = 0$ ) (i.e., dead), and  $t_n \in \mathbb{R}^+$  represents the overall survival time (in months). These two components make up its set of labels  $\mathbf{Y}_n = (c_n, t_n)$ . Following the previous setting [5, 33], the continuous survival time would be discretized into  $I_t$  time intervals corresponding to  $I_t$  risk bands. As a result, the label set  $(c_n, t_n)$  can be re-written as  $y_n$ , resulting in  $2I_t$  labels.

Given a set of predicted hazard probabilities  $\mathbf{h}_n$  across all time intervals, the hazard probability  $\mathbf{h}_n^{(j)}$  represents the probability of death event occurring at the  $j$ -th time interval. Then, the cumulative survival probability for each time interval can be estimated as follows:

$$S_n^{(j)} = \prod_{z=1}^j (1 - \mathbf{h}_n^{(z)}) \quad (1)$$

Following previous works [33, 39], given the ground truth time interval  $\tau$ , we use the NLL loss [36] for survival prediction, where  $N$  is the sample number of the training set:

$$\begin{aligned} \mathcal{L}_{surv} = - \sum_{n=1}^N & [c_n \log S_n^{(\tau)} + (1 - c_n) \log S_n^{(\tau-1)} \\ & + (1 - c_n) \log \mathbf{h}_n^{(\tau)}] \end{aligned} \quad (2)$$

### 3.2. Stage 1: Unimodal Prompting (UniPro)

Given a WSI  $\mathbf{X}_n^p = \{\mathbf{x}_{n,i}^p\}_{i=1}^{M_p}$  or a bag of genomic pathways  $\mathbf{X}_n^g = \{\mathbf{x}_{n,i}^g\}_{i=1}^{M_g}$ , we formulate their learning process as a MIL task. Inspired by CoOp [41] employing a CLIP-style architecture, we adapt it to the MIL setting to learn how to characterize each modality using a set of learnable prompts for modality-specific knowledge.

In terms of pathological WSIs data, following the common setting of the WSI processing [25], as shown in the UniPro-P of Fig 2, we first employ a pretrained and frozen patch encoder  $g_E(\cdot)$  to embed every patch images  $\mathbf{x}_{n,i}^p$  from a WSI into an instance-level embedding  $p_n^i = g_E(\mathbf{x}_{n,i}^p) \in \mathbb{R}^d$ , where  $d$  is the patch feature dimension. To align pathology features with the text space, we apply an adapter  $f_p(\cdot)$  for each patch feature to get the aligned patch feature  $\mathbf{p}_n^i = f_p(g_E(\mathbf{x}_{n,i}^p)) \in \mathbb{R}^D$ , implemented by a linear layer followed by ReLU [2].

Text-wise, the input comprises three components: pathology context tokens, prefix tokens and classname tokens. For classname tokens  $[C]_{1 \dots s}$ , we map every time interval of overall survival into a unique description, such as “median risk”, and denote the censorship status by “alive” or “dead”. The prefix tokens  $[\text{PREFIX}]_{1 \dots m}$  briefly describe the modality, e.g., “This is a pathology slide image from the patient with overall survival of  $[C]_{1 \dots s}$ ”. Prefix and classname tokens are obtained using a frozen Tokenizer pretrained on a large-scale biomedical corpus to embed these words. To learn how to describe the modality for

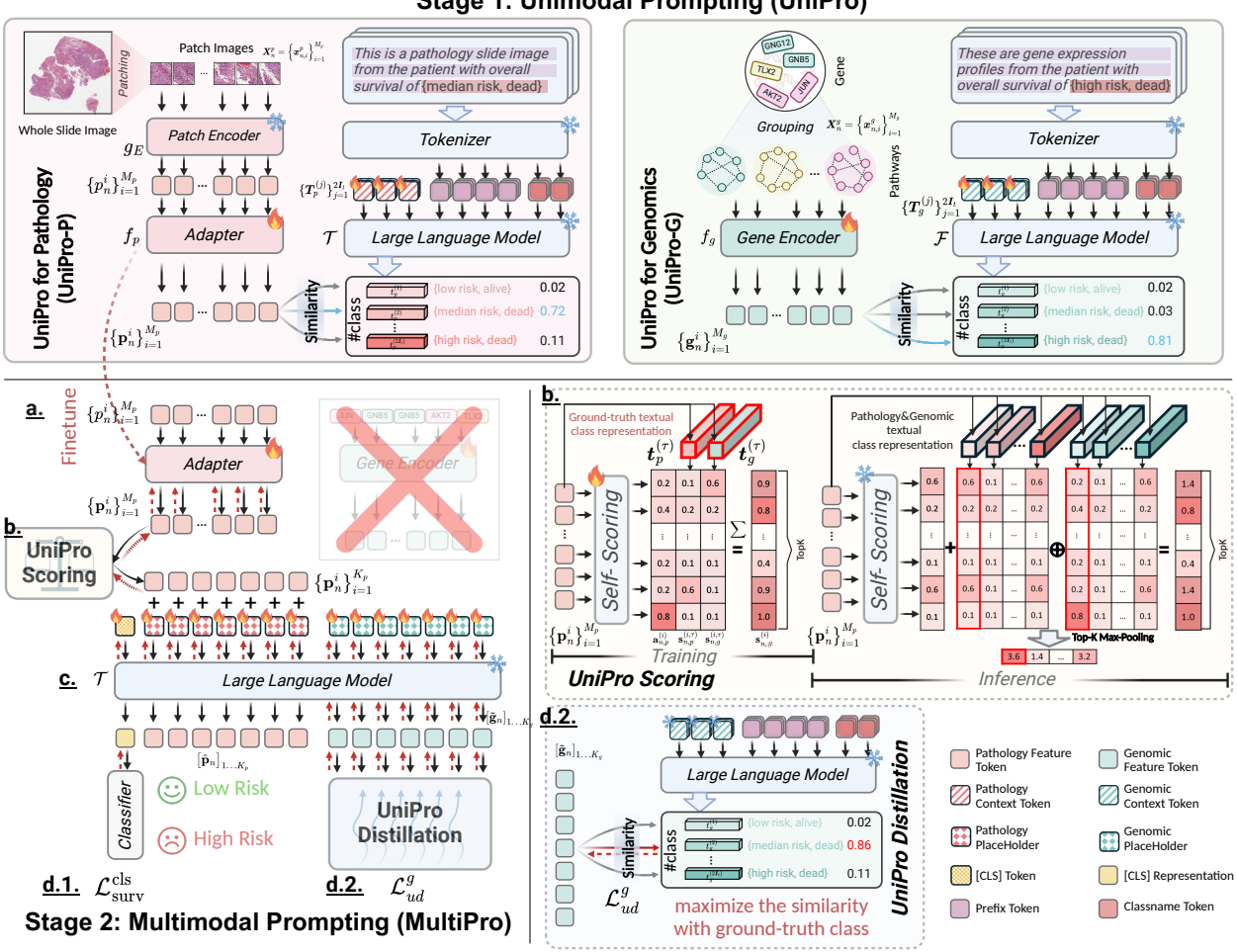


Figure 2. **Overview of DisPro.** Stage 1: Unimodal Prompting aims to distill the knowledge distribution for each modality and prepare to supplement modality-specific knowledge for the missing modality. Stage 2: Multimodal Prompting utilizes the available modality as prompts to infer the representations of the missing one, compensating for modality-common knowledge. Simultaneously, the learned UniPro of Stage 1 supervises the learning of imputed representations to compensate for modality-specific knowledge. UniPro Scoring re-uses learned prompts to assist the LLM in capturing modality-common knowledge by selecting discriminative and relevant tokens.

a specific risk band (class), we attach a set of learnable context tokens  $[P]_{1 \dots k}$  to prefix and classname tokens:

$$T_p = [P]_1 \dots [P]_k [\text{PREFIX}]_1 \dots [\text{PREFIX}]_m [C]_1 \dots [C]_s \quad (3)$$

where  $k, m$  and  $s$  are the token numbers of pathology context tokens, prefix words and classname words, respectively. Each token is a vector with the same dimension  $D$  as word embeddings of the LLM (i.e., 768 for BERT). In this way, we can design input tokens for each risk band:

$$T_p^{(j)} = [P]_1^{(j)} \dots [P]_k^{(j)} [\text{PREFIX}]_1 \dots [\text{PREFIX}]_m [C]_1^{(j)} \dots [C]_s^{(j)} \quad (4)$$

in which  $j \in [1, 2I_t]$  and prefix tokens are shared across all risk bands. By forwarding  $T_p^{(j)}$  of each class to the text encoder  $\mathcal{T}(\cdot)$  (i.e., LLM), we can obtain a global textual class representation  $t_p^{(j)} \in \mathbb{R}^D$  for every class.

In the MIL setting, to obtain the predicted probability for each class, we can use topK patches to produce the slide-level prediction based on similarity scores. To this end, we first compute the similarity score between every instance and every class:

$$s_{n,p}^{(i,j)} = \mathbf{p}_n^i \cdot t_p^{(j)} \quad (5)$$

As a result, we can get a similarity matrix  $\mathcal{S}_{n,p} \in \mathbb{R}^{M_p \times 2I_t}$  for a WSI. Then, we apply a TopK max-pooling operator  $h(\cdot)$  to obtain the slide-level predictions, depending on top-K similarities for each class:

$$h(\mathcal{S}_{n,p}) = \frac{1}{K} \left[ \sum_{i=1}^K \hat{s}_{n,p}^{(i,1)}, \sum_{i=1}^K \hat{s}_{n,p}^{(i,2)}, \dots, \sum_{i=1}^K \hat{s}_{n,p}^{(i,2I_t)} \right] \quad (6)$$

where  $\hat{s}_{n,p}$  is the sorted  $s_{n,p}$  in a descending order across all instances. Next, we can get a set of hazard probabilities

$\mathbf{h}_n^p$  across all time intervals through a sigmoid function.

$$\mathbf{h}_n^p = \text{Sigmoid}(h(\mathcal{S}_{n,p})) \quad (7)$$

By computing the survival loss according to Eq. 2 and back-forwarding gradients, we can optimize the modality adapter and learnable prompts consisting of context tokens.

Similarly, we acquire the set of hazard probabilities  $\mathbf{h}_n^g$  for genomic pathways and optimize its learnable prompts  $\mathbf{T}_g$  and gene encoder  $f_g(\cdot)$ . Here we use the subscript  $p$  and  $g$  to represent pathology and genomic data. Every pathway is also encoded into a  $D$ -dimensional embedding.

### 3.3. Stage 2: Multimodal Prompting (MultiPro)

In this stage, we aim to leverage LLMs' strong inference ability and robustness to missing modalities to predict the representation of missing modalities, as shown in the MultiPro of Fig. 2.

To simplify explanations, we take the example input of pathology available and genomics being missing. By prompting the LLM with available pathology data, the Bert-style LLM can capture modality-common knowledge for genomics due to its nature of self-attention. To compensate for modality-specific knowledge, we re-use the unimodal prompts  $\mathbf{T}_g$  learned in stage 1 with all remaining samples available of genomics data to supervise the learning of imputed representations, where unimodal prompts characterize the knowledge distribution of an individual modality.

To this end, we first need to construct an interleaved input for the learning of modality-common information. To fully leverage the capabilities of LLMs, every modality are supposed to be embedded into the aligned text space. Consequently, we re-use the aligned modality adapter or encoder learned in the first stage to embed each modality, and we continue to finetune them in the second stage. Note that the LLM used in stage 2 is the same as the one in stage 1. As a result, we can get a bag of aligned feature tokens  $\{\mathbf{p}_n^i\}_{i=1}^{M_p}$  or  $\{\mathbf{g}_n^i\}_{i=1}^{M_g}$  for pathology and genomic data, respectively. Here we assume genomic data  $\{\tilde{\mathbf{g}}_n^i\}_{i=1}^{M_g}$  is missing.

Due to the limitation of input length for general LLMs (e.g., 512 for Bert-style LLMs) and high information redundancy in WSIs or genomic pathways [27, 39], more discriminative and relevant feature tokens are expected to be selected for better capturing modality-common knowledge. Therefore, we propose a UniPro Scoring module by re-using UniPro as a grader to estimate a relevance score for each feature token.

**UniPro Scoring.** The score of every feature token is determined by three parts: relevance scores estimated by UniPro-P and UniPro-G, and self-scoring, as shown in Fig. 2.

Given a set of pathology feature tokens  $\{\mathbf{p}_n^i\}_{i=1}^{M_p}$ , to obtain discriminative tokens, we compute the similarity score  $s_{n,p}^{(i,\tau)}$  between the ground-truth textual class representation of  $t_p^{(\tau)}$  and each feature token  $\mathbf{p}_n^i$  by re-using Eq. 5.

Through the sigmoid function, we can get the score  $\mathbf{s}_{n,p}^{(i,\tau)}$  estimated by UniPro-P. To capture cross-modal modality-common information for better compensation of missing modality, we similarly obtain the score  $\mathbf{s}_{n,g}^{(i,\tau)}$  estimated by UniPro-G. Since textual class representations of UniPro are fixed once finishing the training of stage 1, the selected tokens will also become fixed accordingly. To make it diverse while dynamically adapting to the current input, we employ a learnable self-scoring mechanism implemented by attention layers [11] to assign a score  $\mathbf{a}_{n,p}^{(i)}$  for each feature token. In the end, the final score  $\mathbf{s}_{n,\#}^{(i)}$  for each feature token can be computed by their summarization:

$$\mathbf{s}_{n,\#}^{(i)} = \mathbf{s}_{n,p}^{(i,\tau)} + \mathbf{s}_{n,g}^{(i,\tau)} + \mathbf{a}_{n,p}^{(i)} \quad (8)$$

For the inference phase when the ground-truth class cannot be accessed, we compute similarity scores with all textual class representations and apply Top-K max-pooling to determine which class  $j$  these tokens belong to:

$$\tau = \arg \max_{j \in [1, 2I_t]} h(\mathcal{S}_{n,p}^{(j)} \oplus \mathcal{S}_{n,g}^{(j)}) \quad (9)$$

where  $\oplus$  refers to the element-wise addition and  $h(\cdot)$  can be computed by Eq. 6.

By selecting feature tokens with the top- $K_p$  largest scores, we can get the input tokens  $\{\mathbf{p}_n^i\}_{i=1}^{K_p}$  for available pathology modality. Then, we employ a set of learnable tokens to act as placeholders  $[H_p]_{1 \dots K_p}$  and  $[H_g]_{1 \dots K_g}$  for pathology and genomic data, where  $K_p$  and  $K_g$  are their token number of the input for the LLM in stage 2, respectively. They are initialized with modality indicators. For the available pathology, we add the selected tokens to its placeholders, leading to the input of pathology  $\{\hat{\mathbf{p}}_n^i\}_{i=1}^{K_p}$ . At last, we concatenate them with placeholders of the missing genomics as well as a [CLS] token, resulting in the final input being forwarded into a LLM  $\mathcal{T}(\cdot)$ :

$$[\text{CLS}][\hat{\mathbf{p}}_n]_{1 \dots K_p}[\tilde{\mathbf{g}}_n]_{1 \dots K_g} = \mathcal{T}([\text{CLS}] \parallel \{\hat{\mathbf{p}}_n^i\}_{i=1}^{K_p} \parallel [H_g]_{1 \dots K_g}) \quad (10)$$

**UniPro Distillation.** To inject modality-specific knowledge for the compensation of missing modality, we utilize UniPro to supervise this process, where UniPro has learned the knowledge distribution regarding the missing modality based on other observed samples in stage 1.

Given the output (Eq. 10) of the LLM in stage 2, we take the part of the missing modality  $[\tilde{\mathbf{g}}_n]_{1 \dots K_g}$  and compute similarity scores  $\tilde{\mathbf{h}}_g$  between  $[\tilde{\mathbf{g}}_n]_{1 \dots K_g}$  and the textual class representation by Eq. 5 - 7. By substituting  $[\tilde{\mathbf{g}}_n]_{1 \dots K_g}$  into the survival loss function of Eq. 2, we can supervise the learning of compensation for the missing modality:

$$\begin{aligned} \mathcal{L}_{ud}^g = & - \sum_{n=1}^{\tilde{N}_g} [c_n \log S_n^{(\tau)} + (1 - c_n) \log S_n^{(\tau-1)} \\ & + (1 - c_n) \log \tilde{\mathbf{h}}_n^{g,(\tau)}] \end{aligned} \quad (11)$$

where  $\tilde{N}_g$  is the number of missing genomic modalities across all data pairs. Similarly, we can get the loss function  $\mathcal{L}_{ud}^p$  when the pathology modality is missing. Lastly, [CLS] token is used for calculating the loss function for survival prediction  $\mathcal{L}_{surv}^{cls}$  in stage 2, and the final loss can be combined linearly with coefficient factors  $\alpha_1$  and  $\alpha_2$ :

$$\mathcal{L} = \mathcal{L}_{surv}^{cls} + \alpha_1 \mathcal{L}_{ud}^p + \alpha_2 \mathcal{L}_{ud}^g \quad (12)$$

## 4. Experiments

### 4.1. Datasets and Settings

**Datasets.** To demonstrate the efficacy of the proposed method, we conducted a series of experiments across five public cancer datasets sourced from The Cancer Genome Atlas (TCGA)<sup>1</sup>. The case number of each dataset is demonstrated next to the dataset name in Tab. 1. Regarding genomic data, we follow the grouping of biological pathways provided by [12] and remove genes absent in the cBioPortal<sup>2</sup> database, resulting in 330 pathways. More details of datasets can be found in supplementary materials.

**Evaluation Settings on Incomplete Modalities.** Following the common setting in previous works [19, 29], to systematically assess performances on various missing settings, we first manually construct a series of missing scenarios under different missing ratios by randomly dropping them for training sets on samples with complete modality pairs. Specifically, we set a total missing rate (60%) for two modalities and then construct 5 combinations for pathology and genomics, i.e.,  $\{(0\%, 60\%), (20\%, 40\%), (30\%, 30\%), (40\%, 20\%), (60\%, 0\%)\}$ . For inference, all methods are evaluated on three scenarios: pathology only, genomics only, and complete modalities. All experiments are conducted on 5-fold cross-validation following previous works [5, 33] in survival prediction, and the concordance index (C-Index) and its standard deviation (std) are reported to evaluate performances. The LLM is implemented by BioBERT-v1.2 [14]. The supplementary materials contain more experiment results and details on the implementation.

### 4.2. Comparisons with SOTAs

We first present unimodal approaches, and SOTA multimodal methods trained with complete modalities (all pathology and genomics data) to serve as the upper bound of current complete modality approaches. Then the average performances on all missing combinations are demonstrated under the total training missing rate of 60%, evaluated on three inference scenarios. Details on various combinations are shown in Fig. 3 and we discuss them in Sec. 4.3. Lastly, we investigate the upper bound of each model tailored to incomplete modalities by training them with all data (without missing data).

From results in Tab. 1, we observed that (1) When applying 60% training missing rate, DisPro consistently outperformed SOTAs across five datasets by a large margin (on average, +2.23% for pathology only, +1.57% for genomics only and 2.33% for complete data). This indicates the superiority of DisPro over the incomplete SOTA methods. (2) When testing on the complete scenario, on 3 out of 5 datasets and overall, DisPro even surpassed the SOTA multimodal survival model (SurvPath) trained on all data. Notably, DisPro achieved this while only utilizing incomplete training data with a 60% missing rate. It suggests that harnessing the powerful capabilities of LLMs is a promising solution for addressing the classical question of survival analysis. (3) When using complete training data, DisPro consistently performed best on average for various test scenarios as well (2.28% on pathology only, 1.33% on genomics only and 2.57% on complete test data). Under the same condition, DisPro further increased by 1.31% compared with the SOTA complete multimodal method, further demonstrating the strong power of LLMs. (4) In contrast to unimodal methods trained on full unimodal datasets, DisPro, using only incomplete multimodal data with a 60% missing rate, achieved superior or similar performance when inferring from individual modalities. This showcases DisPro’s efficient utilization of multimodal data.

### 4.3. Ablation Study

**Component Validation.** In Tab. 2, we ablate each component in our method to investigate their effectiveness. (1) To demonstrate how the LLM performs on missing modalities without any prompts, we establish a **baseline** by employing a linear classifier head on the same LLM and randomly selecting feature tokens for its input. Results show that the performance significantly decreased by 2.62% on pathology only, 1.55% on genomics only and 2.05% on complete test data. This indicates the importance of appropriate prompts for LLMs. (2) When supplementing modality-specific information for missing modalities, the performance (+UD) consistently improves on all datasets and increases by around +1% on various inference settings, which validates the effectiveness of compensating for modality-specific knowledge of the missing modality. (3) When reusing UniPro to select relevant tokens (+US), the performance increased by about +1% overall, which benefits from the assistance of US in learning modality-common knowledge from WSIs and genes with high redundancy.

**Various Missing Scenarios.** To illustrate how incomplete multimodal approaches handle varying missing settings, we display different combinations of training missing rates for each inference scenario, as shown in Fig. 3. Results showcase that DisPro achieved considerably consistent performance superiority in various missing settings over other incomplete multimodal approaches by a clear margin.

<sup>1</sup><https://portal.gdc.cancer.gov/>

<sup>2</sup><https://www.cbiportal.org/>

Training MiRate	Test		Methods	BLCA (372)	BRCA (1007)	COADREAD (533)	LUAD (443)	UCEC (478)	Avg
	P	G							
N/A	•	○	†TransMIL [25]	0.5903 $\pm$ 0.025	0.6671 $\pm$ 0.054	0.6093 $\pm$ 0.018	0.6195 $\pm$ 0.035	<b>0.6978<math>\pm</math>0.046</b>	0.6368
			†CoOp_BioBert [41]	<b>0.6014<math>\pm</math>0.047</b>	<b>0.6784<math>\pm</math>0.032</b>	<b>0.6681<math>\pm</math>0.026</b>	<b>0.6543<math>\pm</math>0.052</b>	0.6791 $\pm$ 0.085	<b>0.6563</b>
	•	●	†SNN [13]	<b>0.6831<math>\pm</math>0.040</b>	0.6567 $\pm$ 0.038	0.6312 $\pm$ 0.058	0.6379 $\pm$ 0.071	<b>0.7267<math>\pm</math>0.073</b>	0.6671
			†CoOp_BioBert [41]	0.6712 $\pm$ 0.036	<b>0.6922<math>\pm</math>0.035</b>	<b>0.6743<math>\pm</math>0.048</b>	<b>0.6514<math>\pm</math>0.065</b>	0.7171 $\pm$ 0.060	<b>0.6812</b>
	•	○	‡MOTCat [33]	0.6274 $\pm$ 0.046	0.6721 $\pm$ 0.038	0.6501 $\pm$ 0.035	0.6753 $\pm$ 0.043	0.7207 $\pm$ 0.074	0.6691
			‡SurvPath [12]	<b>0.6572<math>\pm</math>0.027</b>	<b>0.7071<math>\pm</math>0.039</b>	<b>0.7079<math>\pm</math>0.048</b>	<b>0.6798<math>\pm</math>0.049</b>	<b>0.7391<math>\pm</math>0.065</b>	<b>0.6982</b>
60%	•	○	COM [24]	0.6024 $\pm$ 0.013	<u>0.6740<math>\pm</math>0.011</u>	<u>0.6779<math>\pm</math>0.014</u>	0.6336 $\pm$ 0.011	0.6985 $\pm$ 0.012	0.6573
			M3Care [37]	<u>0.6208<math>\pm</math>0.014</u>	0.6690 $\pm$ 0.018	0.6570 $\pm$ 0.023	0.6219 $\pm$ 0.007	0.7031 $\pm$ 0.012	0.6543
			MUSE [31]	0.6207 $\pm$ 0.013	0.6514 $\pm$ 0.014	0.6547 $\pm$ 0.009	0.6354 $\pm$ 0.012	<u>0.7048<math>\pm</math>0.023</u>	0.6534
			MAP [15]	0.5918 $\pm$ 0.012	0.6278 $\pm$ 0.006	0.5965 $\pm$ 0.017	0.6489 $\pm$ 0.020	0.6929 $\pm$ 0.021	0.6316
			DisPro (Ours)	<b>0.6319<math>\pm</math>0.014</b>	<b>0.6895<math>\pm</math>0.011</b>	<b>0.6880<math>\pm</math>0.010</b>	<b>0.6612<math>\pm</math>0.014</b>	<b>0.7272<math>\pm</math>0.018</b>	<b>0.6796</b>
	○	●	COM [24]	0.6415 $\pm$ 0.016	<u>0.6653<math>\pm</math>0.018</u>	<u>0.6593<math>\pm</math>0.030</u>	0.6456 $\pm$ 0.008	0.7105 $\pm$ 0.007	0.6645
			M3Care [37]	<u>0.6420<math>\pm</math>0.015</u>	0.6642 $\pm$ 0.029	0.6491 $\pm$ 0.008	0.6462 $\pm$ 0.012	0.7032 $\pm$ 0.013	0.6609
			MUSE [31]	0.6299 $\pm$ 0.012	0.6427 $\pm$ 0.025	0.6391 $\pm$ 0.023	0.6462 $\pm$ 0.010	0.6893 $\pm$ 0.027	0.6494
			MAP [15]	0.5937 $\pm$ 0.016	0.6269 $\pm$ 0.006	0.5971 $\pm$ 0.017	0.6442 $\pm$ 0.009	0.6934 $\pm$ 0.018	0.6311
			DisPro (Ours)	<b>0.6547<math>\pm</math>0.012</b>	<b>0.6841<math>\pm</math>0.018</b>	<b>0.6804<math>\pm</math>0.024</b>	<b>0.6548<math>\pm</math>0.012</b>	<b>0.7271<math>\pm</math>0.017</b>	<b>0.6802</b>
	•	●	COM [24]	0.6192 $\pm$ 0.013	0.6846 $\pm$ 0.009	<u>0.6874<math>\pm</math>0.005</u>	0.6548 $\pm$ 0.012	0.7136 $\pm$ 0.016	0.6719
			M3Care [37]	<u>0.6513<math>\pm</math>0.005</u>	<u>0.6951<math>\pm</math>0.024</u>	0.6698 $\pm$ 0.016	0.6491 $\pm$ 0.013	<u>0.7288<math>\pm</math>0.011</u>	<u>0.6788</u>
			MUSE [31]	0.6207 $\pm$ 0.012	0.6555 $\pm$ 0.013	0.6539 $\pm$ 0.012	0.6415 $\pm$ 0.008	0.7164 $\pm$ 0.013	0.6576
			MAP [15]	0.5906 $\pm$ 0.013	0.6277 $\pm$ 0.004	0.5990 $\pm$ 0.016	<u>0.6625<math>\pm</math>0.008</u>	0.6901 $\pm$ 0.018	0.6340
			DisPro (Ours)	<b>0.6638<math>\pm</math>0.006</b>	<b>0.7219<math>\pm</math>0.015</b>	<b>0.7029<math>\pm</math>0.016</b>	<b>0.6741<math>\pm</math>0.007</b>	<b>0.7476<math>\pm</math>0.020</b>	<b>0.7021</b>
0%	•	○	COM [24]	0.6154 $\pm$ 0.041	<u>0.6871<math>\pm</math>0.027</u>	<u>0.6925<math>\pm</math>0.044</u>	0.6427 $\pm$ 0.046	0.6806 $\pm$ 0.061	0.6637
			M3Care [37]	<u>0.6268<math>\pm</math>0.024</u>	0.6775 $\pm$ 0.016	0.6850 $\pm$ 0.052	0.6299 $\pm$ 0.038	0.6964 $\pm$ 0.061	0.6631
			MUSE [31]	0.6208 $\pm$ 0.026	0.6767 $\pm$ 0.040	0.6710 $\pm$ 0.041	0.6253 $\pm$ 0.041	<u>0.7099<math>\pm</math>0.063</u>	0.6607
			MAP [15]	0.6205 $\pm$ 0.033	0.6300 $\pm$ 0.053	0.5930 $\pm$ 0.065	<u>0.6662<math>\pm</math>0.055</u>	0.6925 $\pm$ 0.064	0.6404
			DisPro (Ours)	<b>0.6315<math>\pm</math>0.028</b>	<b>0.6945<math>\pm</math>0.044</b>	<b>0.7216<math>\pm</math>0.028</b>	<b>0.6747<math>\pm</math>0.052</b>	<b>0.7104<math>\pm</math>0.056</b>	<b>0.6865</b>
	○	●	COM [24]	0.6681 $\pm$ 0.030	<u>0.6966<math>\pm</math>0.047</u>	<u>0.6770<math>\pm</math>0.024</u>	0.6454 $\pm$ 0.050	<u>0.7095<math>\pm</math>0.059</u>	0.6793
			M3Care [37]	<u>0.6706<math>\pm</math>0.039</u>	0.6611 $\pm$ 0.040	0.6563 $\pm$ 0.021	0.6512 $\pm$ 0.061	0.7047 $\pm$ 0.060	0.6688
			MUSE [31]	0.6256 $\pm$ 0.029	0.6401 $\pm$ 0.024	0.6208 $\pm$ 0.030	0.6547 $\pm$ 0.075	0.6824 $\pm$ 0.039	0.6447
			MAP [15]	0.6093 $\pm$ 0.026	0.6305 $\pm$ 0.051	0.5842 $\pm$ 0.065	<u>0.6653<math>\pm</math>0.045</u>	0.6841 $\pm$ 0.064	0.6347
			DisPro (Ours)	<b>0.6745<math>\pm</math>0.039</b>	<b>0.6996<math>\pm</math>0.028</b>	<b>0.7000<math>\pm</math>0.021</b>	<b>0.6751<math>\pm</math>0.068</b>	<b>0.7140<math>\pm</math>0.060</b>	<b>0.6926</b>

Table 1. C-Index of Comparison to SOTA models on 5 survival cancer datasets. “MiRate” represents Missing Rate. “P” and “G” indicate Pathology and Genomics, respectively. ○ means the modality is missing, while ● refers to the available modality. † and ‡ indicate using all unimodal and complete multimodal data, respectively, while the rest models are for missing modalities. The best results are in **bold**. The second-best results are underlined.

## 5. Conclusion

This work proposed a Distilled Prompt Learning (DisPro) framework to unlock the potential of LLMs for incomplete multimodal learning by two-stage prompting, in which Unimodal Prompting (UniPro) and Multimodal Prompting (MultiPro) were proposed for supplementing modality-specific and modality-common knowledge for missing modalities. In the first stage, UniPro extended CoOp

into the MIL setting and distilled knowledge distribution to a set of learnable prompts for each modality, which prepped for compensation of modality-specific knowledge. In the second stage, considering available modalities as prompts, we leveraged an LLM to impute common knowledge for missing modalities. To inject the specific knowledge of missing modalities, the distilled prompts in UniPro are used to supervise the learning of imputing representations for missing modalities, leading to more

Variants	Test		Modules		BLCA (372)	BRCA (1007)	COADREAD (533)	LUAD (443)	UCEC (478)	Avg
	P	G	US	UD						
baseline	●	○			0.6068 $\pm$ 0.021	0.6668 $\pm$ 0.006	0.6583 $\pm$ 0.012	0.6270 $\pm$ 0.018	0.7081 $\pm$ 0.019	0.6534
+ UD	●	○		✓	0.6213 $\pm$ 0.010	0.6829 $\pm$ 0.008	0.6740 $\pm$ 0.022	0.6327 $\pm$ 0.018	0.7152 $\pm$ 0.011	0.6652
+ US	●	○	✓		0.6285 $\pm$ 0.021	0.6884 $\pm$ 0.016	0.6653 $\pm$ 0.026	0.6546 $\pm$ 0.013	0.7203 $\pm$ 0.007	0.6714
DisPro (full)	●	○	✓	✓	<b>0.6319<math>\pm</math>0.014</b>	<b>0.6895<math>\pm</math>0.011</b>	<b>0.6880<math>\pm</math>0.010</b>	<b>0.6612<math>\pm</math>0.014</b>	<b>0.7272<math>\pm</math>0.018</b>	<b>0.6796</b>
baseline	○	●			0.6435 $\pm$ 0.016	0.6605 $\pm$ 0.033	0.6601 $\pm$ 0.018	0.6467 $\pm$ 0.016	0.7127 $\pm$ 0.007	0.6647
+ UD	○	●		✓	0.6473 $\pm$ 0.017	0.6836 $\pm$ 0.014	0.6707 $\pm$ 0.022	0.6420 $\pm$ 0.020	0.7226 $\pm$ 0.013	0.6732
+ US	○	●	✓		0.6452 $\pm$ 0.020	0.6666 $\pm$ 0.017	0.6763 $\pm$ 0.023	0.6471 $\pm$ 0.023	0.7151 $\pm$ 0.009	0.6701
DisPro (full)	○	●	✓	✓	<b>0.6547<math>\pm</math>0.012</b>	<b>0.6841<math>\pm</math>0.018</b>	<b>0.6804<math>\pm</math>0.024</b>	<b>0.6548<math>\pm</math>0.012</b>	<b>0.7271<math>\pm</math>0.017</b>	<b>0.6802</b>
baseline	●	●			0.6522 $\pm$ 0.010	0.7075 $\pm$ 0.012	0.6785 $\pm$ 0.020	0.6541 $\pm$ 0.009	0.7157 $\pm$ 0.003	0.6816
+ UD	●	●		✓	0.6585 $\pm$ 0.007	0.7194 $\pm$ 0.013	0.6963 $\pm$ 0.009	0.6635 $\pm$ 0.014	0.7250 $\pm$ 0.012	0.6926
+ US	●	●	✓		0.6593 $\pm$ 0.008	0.7125 $\pm$ 0.010	0.7005 $\pm$ 0.018	0.6717 $\pm$ 0.007	0.7274 $\pm$ 0.010	0.6943
DisPro (full)	●	●	✓	✓	<b>0.6638<math>\pm</math>0.006</b>	<b>0.7219<math>\pm</math>0.015</b>	<b>0.7029<math>\pm</math>0.016</b>	<b>0.6741<math>\pm</math>0.007</b>	<b>0.7476<math>\pm</math>0.020</b>	<b>0.7021</b>

Table 2. **C-Index of Ablation Study on the Setting of 60% Training Missing Rate.** “US” and “UD” refer to the UniPro Scoring and UniPro Distillation modules, respectively. “P” and “G” indicate Pathology and Genomics, respectively. ○ means the modality is missing, while ● refers to the available modality.

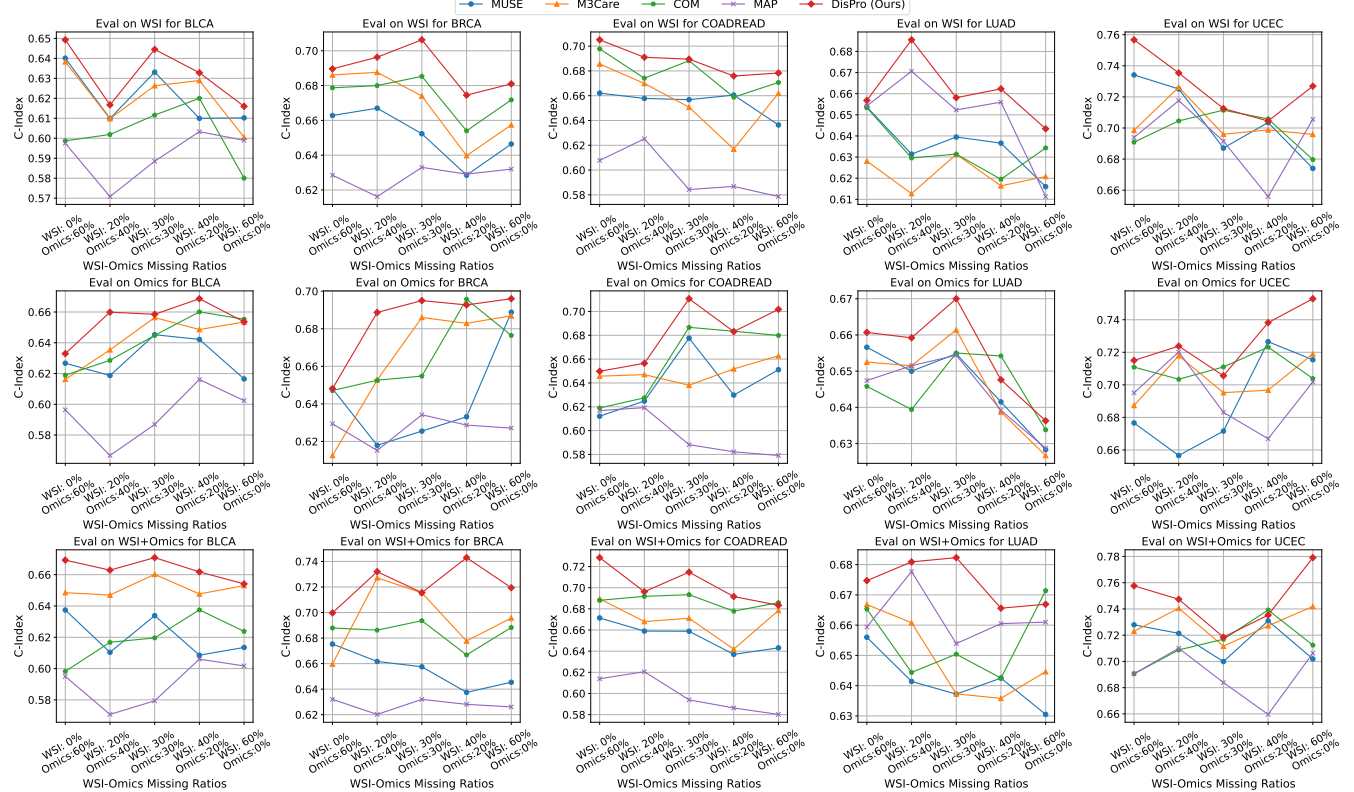


Figure 3. Performance on various combinations under 60% training missing rate for different test scenarios.

comprehensive knowledge compensation in incomplete multimodal learning. Extensive experiments on five cancer benchmark datasets demonstrated the effectiveness of the proposed method over state-of-the-art approaches.

## References

- [1] Som S Biswas. Role of chat gpt in public health. *Annals of biomedical engineering*, 51(5):868–869, 2023. 2
- [2] Jason Brownlee. A gentle introduction to the rectified linear unit (relu). *Machine learning mastery*, 6, 2019. 3

[3] Agisilaos Chartsias, Thomas Joyce, Mario Valerio Giufrida, and Sotirios A Tsaftaris. Multimodal mr synthesis via modality-invariant latent representation. *IEEE transactions on medical imaging*, 37(3):803–814, 2017. 1

[4] Jiayi Chen and Aidong Zhang. Hgmf: heterogeneous graph-based fusion for multimodal data with incompleteness. In *Proceedings of the 26th ACM SIGKDD international conference on knowledge discovery & data mining*, pages 1295–1305, 2020. 1, 2

[5] Richard J Chen, Ming Y Lu, Wei-Hung Weng, Tiffany Y Chen, Drew FK Williamson, Trevor Manz, Maha Shady, and Faisal Mahmood. Multimodal co-attention transformer for survival prediction in gigapixel whole slide images. In *Proceedings of the IEEE/CVF International Conference on Computer Vision*, pages 4015–4025, 2021. 1, 3, 6

[6] Florinel-Alin Croitoru, Vlad Hondu, Radu Tudor Ionescu, and Mubarak Shah. Diffusion models in vision: A survey. *IEEE Transactions on Pattern Analysis and Machine Intelligence*, 45(9):10850–10869, 2023. 2

[7] Yuhang Ding, Xin Yu, and Yi Yang. Rfnet: Region-aware fusion network for incomplete multi-modal brain tumor segmentation. In *Proceedings of the IEEE/CVF international conference on computer vision*, pages 3975–3984, 2021. 1, 2

[8] Zhou et al. Cross-modal translation and alignment for survival analysis. In *ICCV*, pages 21485–21494, 2023. 1, 3

[9] Michael Gadermayr and Maximilian Tschuchnig. Multiple instance learning for digital pathology: A review of the state-of-the-art, limitations & future potential. *Computerized Medical Imaging and Graphics*, page 102337, 2024. 2

[10] Mohammad Hamghalam, Alejandro F Frangi, Baiying Lei, and Amber L Simpson. Modality completion via gaussian process prior variational autoencoders for multi-modal glioma segmentation. In *Medical Image Computing and Computer Assisted Intervention–MICCAI 2021: 24th International Conference, Strasbourg, France, September 27–October 1, 2021, Proceedings, Part VII 24*, pages 442–452. Springer, 2021. 2

[11] Maximilian Ilse, Jakub Tomczak, and Max Welling. Attention-based deep multiple instance learning. In *International conference on machine learning*, pages 2127–2136. PMLR, 2018. 2, 5

[12] Guillaume Jaume, Anurag Vaidya, Richard J Chen, Drew FK Williamson, Paul Pu Liang, and Faisal Mahmood. Modeling dense multimodal interactions between biological pathways and histology for survival prediction. In *Proceedings of the IEEE/CVF Conference on Computer Vision and Pattern Recognition*, pages 11579–11590, 2024. 3, 6, 7

[13] Günter Klambauer, Thomas Unterthiner, Andreas Mayr, and Sepp Hochreiter. Self-normalizing neural networks. *Advances in neural information processing systems*, 30, 2017. 7

[14] Jinyuk Lee, Wonjin Yoon, Sungdong Kim, Donghyeon Kim, Sunkyu Kim, Chan Ho So, and Jaewoo Kang. Biobert: a pre-trained biomedical language representation model for biomedical text mining. *Bioinformatics*, 36(4):1234–1240, 2020. 6

[15] Yi-Lun Lee, Yi-Hsuan Tsai, Wei-Chen Chiu, and Chen-Yu Lee. Multimodal prompting with missing modalities for visual recognition. In *Proceedings of the IEEE/CVF Conference on Computer Vision and Pattern Recognition*, pages 14943–14952, 2023. 2, 7

[16] Bin Li, Yin Li, and Kevin W Eliceiri. Dual-stream multiple instance learning network for whole slide image classification with self-supervised contrastive learning. In *Proceedings of the IEEE/CVF conference on computer vision and pattern recognition*, pages 14318–14328, 2021. 3

[17] Chunyuan Li, Cliff Wong, Sheng Zhang, Naoto Usuyama, Haotian Liu, Jianwei Yang, Tristan Naumann, Hoifung Poon, and Jianfeng Gao. Llava-med: Training a large language-and-vision assistant for biomedicine in one day. *Advances in Neural Information Processing Systems*, 36, 2024. 2

[18] Han Liu, Yubo Fan, Hao Li, Jiacheng Wang, Dewei Hu, Can Cui, Ho Hin Lee, Huahong Zhang, and Ipek Oguz. Mod-drop++: A dynamic filter network with intra-subject co-training for multiple sclerosis lesion segmentation with missing modalities. In *International Conference on Medical Image Computing and Computer-Assisted Intervention*, pages 444–453. Springer, 2022. 2

[19] Mengmeng Ma, Jian Ren, Long Zhao, Sergey Tulyakov, Cathy Wu, and Xi Peng. Smil: Multimodal learning with severely missing modality. In *Proceedings of the AAAI Conference on Artificial Intelligence*, pages 2302–2310, 2021. 2, 6

[20] Xiangxi Meng, Kaicong Sun, Jun Xu, Xuming He, and Dinggang Shen. Multi-modal modality-masked diffusion network for brain mri synthesis with random modality missing. *IEEE Transactions on Medical Imaging*, 2024. 1, 2

[21] Muhammad Khalid Khan Niazi, Anil V Parwani, and Metin N Gurcan. Digital pathology and artificial intelligence. *The lancet oncology*, 20(5):e253–e261, 2019. 3

[22] Zhenyuan Ning, Denghui Du, Chao Tu, Qianjin Feng, and Yu Zhang. Relation-aware shared representation learning for cancer prognosis analysis with auxiliary clinical variables and incomplete multi-modality data. *IEEE Transactions on Medical Imaging*, 41(1):186–198, 2021. 2

[23] Fatih Ozsolak and Patrice M Milos. Rna sequencing: advances, challenges and opportunities. *Nature reviews genetics*, 12(2):87–98, 2011. 3

[24] Shuwei Qian and Chongjun Wang. Com: Contrastive masked-attention model for incomplete multimodal learning. *Neural Networks*, 162:443–455, 2023. 7

[25] Zhuchen Shao, Hao Bian, Yang Chen, Yifeng Wang, Jian Zhang, Xiangyang Ji, et al. Transmil: Transformer based correlated multiple instance learning for whole slide image classification. *Advances in neural information processing systems*, 34:2136–2147, 2021. 3, 7

[26] Anmol Sharma and Ghassan Hamarneh. Missing mri pulse sequence synthesis using multi-modal generative adversarial network. *IEEE transactions on medical imaging*, 39(4):1170–1183, 2019. 1

[27] Andrew H Song, Richard J Chen, Guillaume Jaume, Anurag Jayant Vaidya, Alexander Baras, and Faisal Mahmood. Multimodal prototyping for cancer survival predic

tion. In *Forty-first International Conference on Machine Learning*, 2024. 1, 2, 3, 5

[28] Rory Stark, Marta Grzelak, and James Hadfield. Rna sequencing: the teenage years. *Nature Reviews Genetics*, 20(11):631–656, 2019. 3

[29] Hu Wang, Yuanhong Chen, Congbo Ma, Jodie Avery, Louise Hull, and Gustavo Carneiro. Multi-modal learning with missing modality via shared-specific feature modelling. In *Proceedings of the IEEE/CVF Conference on Computer Vision and Pattern Recognition*, pages 15878–15887, 2023. 6

[30] Tianyu Wu, Shizhu He, Jingping Liu, Siqi Sun, Kang Liu, Qing-Long Han, and Yang Tang. A brief overview of chat-gpt: The history, status quo and potential future development. *IEEE/CAA Journal of Automatica Sinica*, 10(5):1122–1136, 2023. 2

[31] Zhenbang Wu, Anant Dadu, Nicholas Tustison, Brian Avants, Mike Nalls, Jimeng Sun, and Faraz Faghri. Multi-modal patient representation learning with missing modalities and labels. In *The Twelfth International Conference on Learning Representations*, 2024. 1, 2, 7

[32] Conghao Xiong, Hao Chen, Hao Zheng, Dong Wei, Yefeng Zheng, Joseph JY Sung, and Irwin King. Mome: Mixture of multimodal experts for cancer survival prediction. In *International Conference on Medical Image Computing and Computer-Assisted Intervention*, pages 318–328. Springer, 2024. 1

[33] Yingxue Xu and Hao Chen. Multimodal optimal transport-based co-attention transformer with global structure consistency for survival prediction. In *Proceedings of the IEEE/CVF International Conference on Computer Vision*, pages 21241–21251, 2023. 1, 3, 6, 7

[34] Shu Yang, Yihui Wang, and Hao Chen. Mambamil: Enhancing long sequence modeling with sequence reordering in computational pathology. In *International Conference on Medical Image Computing and Computer-Assisted Intervention*, pages 296–306. Springer, 2024. 2

[35] Yixiao Yuan, Yawen Huang, and Yi Zhou. Rethinking a unified generative adversarial model for mri modality completion. In *International Conference on Medical Image Computing and Computer-Assisted Intervention*, pages 143–153. Springer, 2023. 2

[36] Shekoufeh Gorgi Zadeh and Matthias Schmid. Bias in cross-entropy-based training of deep survival networks. *IEEE transactions on pattern analysis and machine intelligence*, 43(9):3126–3137, 2020. 3

[37] Chaohe Zhang, Xu Chu, Liantao Ma, Yinghao Zhu, Yasha Wang, Jiangtao Wang, and Junfeng Zhao. M3care: Learning with missing modalities in multimodal healthcare data. In *Proceedings of the 28th ACM SIGKDD Conference on Knowledge Discovery and Data Mining*, pages 2418–2428, 2022. 1, 2, 7

[38] Hongrun Zhang, Yanda Meng, Yitian Zhao, Yihong Qiao, Xiaoyun Yang, Sarah E Coupland, and Yalin Zheng. Dtfdmil: Double-tier feature distillation multiple instance learning for histopathology whole slide image classification. In *Proceedings of the IEEE/CVF conference on computer vision and pattern recognition*, pages 18802–18812, 2022. 3

[39] Yilan Zhang, Yingxue Xu, Jianqi Chen, Fengying Xie, and Hao Chen. Prototypical information bottlenecking and disentangling for multimodal cancer survival prediction. In *The Twelfth International Conference on Learning Representations*, 2024. 1, 2, 3, 5

[40] Huajun Zhou, Fengtao Zhou, Chenyu Zhao, Yingxue Xu, Luyang Luo, and Hao Chen. Multimodal data integration for precision oncology: Challenges and future directions. *arXiv preprint arXiv:2406.19611*, 2024. 1, 2

[41] Kaiyang Zhou, Jingkang Yang, Chen Change Loy, and Ziwei Liu. Learning to prompt for vision-language models. *International Journal of Computer Vision*, 130(9):2337–2348, 2022. 2, 3, 7